

**ELECTRICAL BREAKDOWN OF GASES IN SUBATMOSPHERIC PRESSURE**

by

Yuxuan Chen

A thesis submitted to the Graduate Faculty of  
Auburn University  
in partial fulfillment of the  
requirements for the Degree of  
Master of Science

Auburn, Alabama  
August 6, 2016

Copyright 2016 by Yuxuan Chen

Approved by

Hulya Kirkici, Chair, Professor of Electrical and Computer Engineering  
Thaddeus Roppel, Member, Associate Professor of Electrical and Computer Engineering  
Shiwen Mao, Member, Professor of Electrical and Computer Engineering

## Abstract

In this study, I present my research on the breakdown phenomenon and discharge characteristics of gaseous dielectrics under DC voltages with different pressures. All of the experiments conducted utilized a point-to-point stainless steel electrode pair separated at 1cm gap distance. The theoretical and experimental breakdown voltage results of different gases are compared. It is observed that different gases has different breakdown voltage under the same experimental conditions and electrode geometry. Besides, the breakdown voltage versus pressure curves of gaseous dielectrics follows the classic Paschen's Law as well. In conclusion, it is shown that the theoretical calculation values are correct. The air and nitrogen have the better insulating properties at selected 1 Torr to 2 Torr range, compared to other gases used in this study.

## Acknowledgement

I am grateful to my advisor Dr. Hulya Kirkici for her patience and guidance. The door to Prof. Kirkici's office was always open whenever I ran into a trouble spot or had a question about my research. I would like to thank Dr. Mao and Dr. Roppel for serving as the committee members.

The graduate peers I would like to thank are Dr. Alper Kara, Mike Moley, and Baha Yakupoglu, for their help during the months of research dedicated to troubleshooting with the experiment setup over and over again.

I am truly grateful for the enormous support from my parents. With their encouragement and help, I eventually finished my thesis and degree.

## Table of Contents

Abstract . . . . .	ii
Acknowledgments . . . . .	iii
List of Tables . . . . .	vi
List of Figures . . . . .	vii
Chapter 1 INTRODUCTION . . . . .	1
Chapter 2 BACKGROUND AND LITERATURE . . . . .	6
2.1 Basic concepts . . . . .	6
2.2 Gas Breakdown mechanisms . . . . .	6
2.2.1 Townsend discharge theory . . . . .	6
2.2.2 Paschen's law . . . . .	8
2.2.3 Streamer Theory of Breakdown . . . . .	11
2.3 High Frequency Breakdown . . . . .	12
2.4 Air and Gas dielectrics Insulation . . . . .	14
2.4.1 Air Insulation Application . . . . .	14
2.4.2 Gas Dielectrics . . . . .	15
2.4.3 Vacuum Surface Flashover . . . . .	16
2.5 Space System Insulation . . . . .	18
Chapter 3 EXPERIMENTAL SETUP AND PROCEDURE . . . . .	19
3.1 Experimental Setup . . . . .	19
3.2 Experimental Procedure . . . . .	23
Chapter 4 RESULTS AND DISCUSSION. . . . .	24

4.1 Theoretical Calculation .....	24
4.2 DC Breakdown Experiments .....	30
4.3 Comparison between Theoretical and Experimental Curves .....	34
4.4 Conclusions .....	38
Chapter 5 RESULTS AND DISCUSSION.....	39
References .....	41

## List of Tables

Table 2.1 Minimum breakdown voltages . . . . .	9
Table 2.2 Five kinds of models for investigation of different power networks . . . . .	15
Table 4.1 Numerical Parameters A and B of Townsend Coefficient $\alpha$ . . . . .	24
Table 4.2 Calculation Process of Air Breakdown Voltage (A=15 1/cm Torr, B=365 V/cm Torr) . . . . .	26
Table 4.3 Calculation Process of Nitrogen Breakdown Voltage (A=10 1/cm Torr, B=310 V/cm Torr) . . . . .	27
Table 4.4 Calculation Process of Helium Breakdown Voltage (A=3 1/cm Torr, B=34 V/cm Torr) . . . . .	28
Table 4.5 Calculation Process of Argon Breakdown Voltage (A=12 1/cm Torr, B=180 V/cm Torr) . . . . .	29

## List of Figures

Figure 2.1 Schematics of gas discharge process . . . . .	7
Figure 2.2 Curve of current versus applied voltage . . . . .	7
Figure 2.3 Paschen's law for breakdown voltages of H <sub>2</sub> , Air and CO <sub>2</sub> . . . . .	10
Figure 2.4 Paschen's curves of different gases under 400 Hz at room temperature . . . . .	11
Figure 2.5 The development of avalanche to a streamer in a uniform field (+= positive ions, -=electrons, ph= photons emitted from the avalanche . . . . .	12
Figure 2.6 Ratio of high-frequency breakdown voltage to static breakdown voltage as a function of frequency for a uniform air gap . . . . .	14
Figure 2.7 The main processes responsible for the production of the charged particles in a gas discharge . . . . .	16
Figure 2.8 Schematic of triple junction in vacuum . . . . .	17
Figure 2.9 The mechanism of gas molecules are desorbed from the surface . . . . .	17
Figure 2.10 The needs for high power level space system . . . . .	18
Figure 3.1 Vacuum Chamber . . . . .	20
Figure 3.2 The schematic of the experiment setup . . . . .	21
Figure 3.3 Point-to-point electrode configuration . . . . .	22
Figure 4.1 Air Breakdown Voltage as a Function of Pressure with Theoretical Data . . . . .	26
Figure 4.2 Nitrogen Breakdown Voltage as a Function of Pressure with Theoretical Data . . . . .	27
Figure 4.3 Helium Breakdown Voltage as a Function of Pressure with Theoretical Data . . . . .	28
Figure 4.4 Argon Breakdown Voltage as a Function of Pressure with Theoretical Data . . . . .	29
Figure 4.5 Voltage (top), light emission (bottom) waveforms of a breakdown event point-to-point electrode geometry for DC voltage at 100 milliTorr . . . . .	30

Figure 4.6 Voltage (top), light emission (bottom) waveforms of a breakdown event point-to-point electrode geometry for DC voltage at 6 Torr .....	31
Figure 4.7 Air Breakdown Voltage as a Function of Pressure with Experimental Data .....	32
Figure 4.8 Nitrogen Breakdown Voltage as a Function of Pressure with Experimental Data .....	32
Figure 4.9 Helium Breakdown Voltage as a Function of Pressure with Experimental Data (a) .....	33
Figure 4.10 Helium Breakdown Voltage as a Function of Pressure with Experimental Data (b) .....	33
Figure 4.11 Argon Breakdown Voltage as a Function of Pressure with Experimental Data .....	34
Figure 4.12 Comparison between Theoretical and Experimental Air Breakdown Voltage Curve (Experimental top, Theoretical bottom) .....	35
Figure 4.13 Comparison between Theoretical and Experimental Nitrogen Breakdown Voltage Curve (Experimental top, Theoretical bottom) .....	35
Figure 4.14 Comparison between Theoretical and Experimental Argon Breakdown Voltage Curve (Experimental top, Theoretical bottom) .....	36
Figure 4.15 Comparison between Theoretical and Experimental Helium Breakdown Voltage Curve (a) first time (b) second time .....	37



# **CHAPTER 1**

## **INTRODUCTION**

Modern electrical industry with high voltage levels, needs the investigation of breakdown characteristics of dielectrics. Aerospace industry, such as aircraft and space station applications, is also requiring much higher power levels nowadays. Switched-mode power supplies offer solution to overcome these challenges. Meanwhile, understandings of the effects of higher voltage levels on insulator breakdown under sub-atmospheric vacuum condition are essential.

The high voltage insulation becomes more and more important in power systems. In order to reduce the losses on transmission lines, higher voltage levels are utilized in many countries. Therefore, the development of high voltage insulation technologies determines the reliability of power supply. Gaseous dielectrics, especially the air, have wide range of applications in power system. Basic requirements for an ideal gaseous insulator are to be cheap, stable, and not produce flammable or toxic materials under prolonged electrical stresses. It should also have high uniform and non-uniform field dielectrics strengths under AC, DC and pulsed power [1].

Air, used as an insulator, is applied in most high-voltage transmission lines and open air circuit-breakers. Under normal circumstances, the air is not conductive and known as an insulator. On the other hand due to the cosmic rays, it normally contains a small amount of charged particles, but the number is extremely low, unable to form a conductive path. However, if the air gap is applied a critical voltage, the current in the air gap will suddenly surge, with apparent light and heat phenomenon at the same time. Then it will suddenly lose insulating properties and a conductive path will be formed. This phenomenon is called the gas discharge. There are two forms of gas discharge, namely breakdown and flashover. The former refers to

the pure air gap discharge, and the latter refers to the gas discharge along a solid surface. Breakdown and flashover are collectively referred as discharge. The gas discharge will only cause a temporary loss of the insulation. Once the discharge is extinguished, it can recover insulation performance, so the gas insulation has a kind of self-recovery insulation property. Air is the cheapest and inexhaustible insulation material. Usually air is used in engineering as the outer insulation of electric equipment and insulation of overhead transmission line, whose breakdown strength is 30kV/cm. In the gas dielectric, in addition to air, large amounts of sulfur hexafluoride are used as insulating medium; sulfur hexafluoride gas is often an internal insulation for electrical equipment.

Compared with other dielectric materials, vacuum theoretically has the strongest dielectric breakdown strength, because there is no residual gas and electron collision in the interelectrode gap. According to Paschen's Law, the sub-atmospheric pressure means much lower breakdown voltage level than atmospheric environment. On the other hand, in vacuum, breakdown voltage can be higher than the atmospheric pressures. In practice, there are absorbed gas and other contaminants exist on the surface of metallic electrodes in vacuum environment. Generally, the residual gas pressure of  $10^{-9}$ - $10^{-12}$  bar exist in what is considered to be the vacuum environment, and it is called "partial vacuum" environment. When certain threshold electric field intensity is reached, electric field will stimulate charge carriers, and breakdown or flashover will occur finally. However, with a suitable design, the vacuum breakdown strength is still better than most of the dielectric materials. This is why vacuum insulation could be used widely in space power systems. It's also the necessity why we study the breakdown characteristics of materials under vacuum condition.

With the advanced developments in aerospace technologies, higher power levels are utilized to satisfy the increasing requirements. The International Space Station (ISS) is using a 160V operation voltage compared to a previous 28V standard voltage, and up to 100kW power

level. But more power means heavier power supply system. Generally, researchers use higher frequency level and more compact components to match the requirements. But this, more compact design brings some insulation failures due to the overstress, incompatible coordination. Therefore, switch mode power supply (SMPS) becomes more favored because of its advantages in compactness and effectiveness. The working frequency of high voltage SMPS in space system is increased from a low range of 60 Hz ~ 400 Hz to radio frequency range of 10 kHz ~ 1 MHz. Thus, SMPS needs a high switching frequency during work. In space systems, high frequency levels enhance the partial discharges and corona, resulting in power loss and degradation, aging or even thermal breakdown of the bulk insulation and components. High frequency also generates electromagnetic interference which disturbs the signal transmissions in space power systems [11]. The dielectric surface composition and the surface charging are affected by the low earth orbit (LEO) plasma and UV irradiation. Also, LEO plasma and UV irradiation generate seed electrons for the breakdown process [2]. The insulation in ground based systems already experience short circuiting, power losses, and impose spurious signals onto communication systems and sensitive sensors due to arcing discharges. In space systems, other environmental factors, in addition to the above failures, such as electrical degradation and flashover at lower voltages might occur due to the molecular and particulate contaminants and outgassing [11]. It is important to clarify the breakdown characteristics when the power supply working with contaminations under such a high frequency operation.

Significantly, vacuum insulation is a well-known technology for space power systems. But it is significantly important in pulsed power systems and has already been researched for decades. The recent advances of large pulsed power devices enhance the necessity for developing vacuum insulation technologies [3].

Also, the flashover voltage value of insulation is much lower than that of breakdown voltage in vacuum. This is a significant constraint on development of more powerful and

compact pulsed power devices [10], because the power density transferred through high-voltage systems is limited by the surface flashover across insulators [2]. This is the starting point of continual surface flashover research in high voltage system insulation under vacuum conditions [10].

Several unpredictable processes, such as partial discharges, corona and volume discharges are detrimental to power systems and devices as they are the constant source of electro-magnetic interference and energy loss. These processes could result in big problems as insulation deterioration and component failure leading to bulk electrical breakdown. Considering the components of power system, the most significant conditions are the geometry of electrode gap (homogeneous, inhomogeneous), type of the field (polar, and unipolar fields), the type of medium (electronegative, atomic, molecular, etc.), the amplitude of applied voltage, and the operation pressure. The breakdown behavior in vacuum is still not clear completely, even it has been extensively studied for decades. Systemic results about the breakdown characteristics of some different gases are needed when DC voltage is applied [6]. Therefore, this study focuses on the breakdown characteristics of gases under DC fields in partial vacuum conditions.

The insulating materials influence the breakdown characteristics of total power system. The most common and popular dielectrics are gases. These dielectrics play an important role in many special high voltage areas. It is valuable to study electrical properties of gases, especially under different conditions, such as the ionization, corona and breakdown process [1].

In recent decades, many researches focus on improving surface insulation strength through doping other metal oxides such as alumina into epoxy. Therefore, high performance composite insulation materials are produced to match more rigorous requirements [5]. The materials made by adding nano-scale particulates into polymer based bulk are called nano-dielectrics. It has been observed that these nano-scale particulates bring significant improvements on the thermal,

electrical and mechanical performances of polymeric materials. Besides, initial findings show that the nano-composite materials have lower electrical conductivity and higher electrical breakdown strength compared to the non-filler added polyamides, These properties make nano-dielectric materials prime candidates for electrical insulation for multi-stress and high repetition rate (high frequency operation) for compact and/or high voltage/power electrical systems.

Insulating materials can be used for both insulation purposes and for charge storage, in addition to other purposes like heat conduction (as in liquids) and mechanical support (as in solids), which make them play a significant role in the design and performance of high voltage power systems [4].

## **CHAPTER 2**

### **BACKGROUND AND LITERATURE**

#### **2.1 Basic concepts**

Breakdown processes have been studied over many decades. There are several important concepts contribute to the formation of breakdown in air. Primary electrons are usually trapped in air, but they will be released by cosmic rays, and background radiation, to collide with neutral molecules after accelerating by strong electrical field. This ionization process is cumulative and promotes the formation of avalanche of electrons, when electrons get enough energy to cause ionization of the background gas. More details about this process will be introduced in next section [17].

#### **2.2 Gas Breakdown mechanisms**

##### **2.2.1 Townsend discharge theory**

The Townsend theory is the earliest theory to explain the breakdown and the gas discharge mechanism. As shown in the Fig. 2.1, two parallel-plate electrodes connected with the positive and negative polarities of DC voltage source respectively, forms a uniform electrical field between them. The free electrons within the gap can be accelerated by the electrical field. They can also be released from the cathode, and collide with the gas molecules to generate more electrons. These electrons are also collide with gas molecules and generate more electrons. Finally, avalanche phenomenon is formed and an electrical conducting pathway through the gas is established. But the electrical field strength and mean free path are important for this discharge process. The electrons must acquire sufficient energy from the applied field. If the electrical field is too small, the electron will not acquire enough velocity to collide with other gas molecule. If the mean free path is too long, the electron will reach anode without

colliding with other gas molecules. On the other hand, if the mean free path is too short, the electrons will lose their accelerated energy in a series non-ionizing collisions.

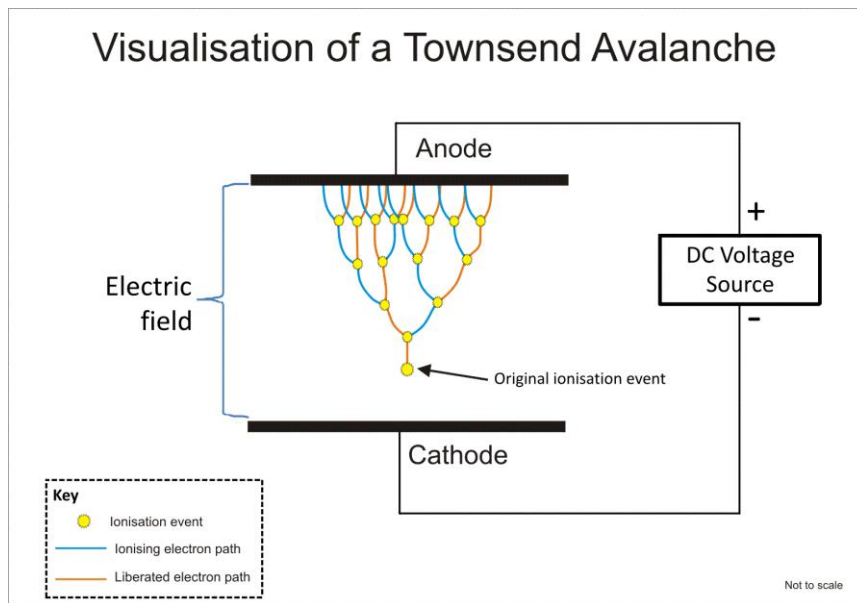


Figure 2.1 Schematics of gas discharge process

The relationship between the current and the applied voltage is shown in Figure 2.2. At the beginning, the current is proportional to the applied voltage closely. After that, there is a saturation stage, the current will reach  $I_0$  for a while. After passing this saturation stage, the current will increase exponentially.

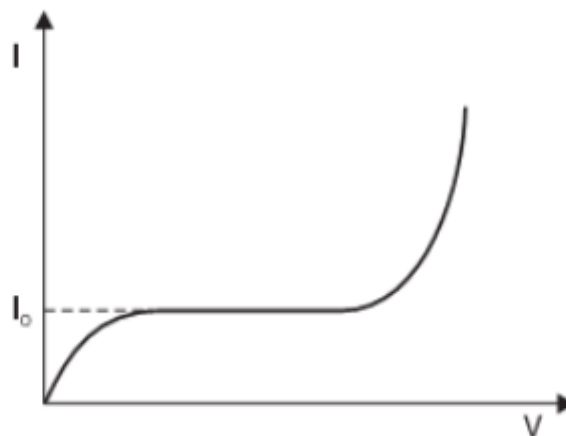


Figure 2.2 Curve of current versus applied voltage

The average number of electrons released by a positive ion is given by

$$\frac{I}{I_0} = \frac{e^{\alpha d}}{1 - \gamma(e^{\alpha d} - 1)} \quad (2.1)$$

Where  $I$  is current flowing in the circuit,  $I_0$  is saturation current,  $\alpha$  is first Townsend coefficient,  $\gamma$  is Townsend secondary ionization coefficient,  $d$  is distance between electrodes. Neglecting the power supply internal resistance, the current becomes infinite if

$$\gamma(e^{\alpha d} - 1) = 1 \quad (2.2)$$

Normally,  $e^{\alpha d} \gg 1$ , and Equation (2.2) is simply expressed as

$$\gamma e^{\alpha d} = 1 \quad (2.3)$$

### 2.2.2 Paschen's law

The Paschen's law essentially describes the breakdown characteristic of a gas in a gap is a nonlinear function of the product of the gas pressure,  $p$ , and the gap distance,  $d$ , and usually written as  $V = f(pd)$ . Actually, the pressure should probably be replaced by the gas density. It has been shown that the gas breakdown criterion is given as  $\gamma(e^{\alpha d} - 1) = 1$ . The coefficients of  $\alpha$  and  $\gamma$  can be determined as functions of the gas pressure  $p$  and the electric field  $E$ .

For parallel plate electrodes  $E = V/d$ ,  $\gamma = f_1(E/p)$  and  $\alpha = pf_2(E/p)$ . Thus, rewriting Equation (2.2) we have

$$f_1(V / pd) \left[ e^{pd f_2(V / pd)} - 1 \right] = 1 \quad (2.4)$$

With understanding the nature of functions  $f_1$  and  $f_2$ , the Equation (2.2) shows a relationship between breakdown voltage and product  $pd$ , and can be rewrite as,

$$V = F(pd) \quad (2.5)$$



This equation is very important for high voltage engineering. It is known as the Paschen's law, and has been experimentally measured for many gas. At low pd values the breakdown voltage is inversely proportional to the pd value, and at high pd values it is directly proportional to the pd parameter. There is a range where breakdown voltage reaches a minimum and it is called the Paschen minimum. These minimum breakdown voltages for different gases are showed in Table 2.1.

Table 2.1 Minimum breakdown voltages

Gas	$V_s$ min (V)	Pd at $V_s$ min (Torr-cm)
Air	327	0.567
Argon	137	0.9
H <sub>2</sub>	273	1.15
Helium	156	4.0
CO <sub>2</sub>	420	0.51
N <sub>2</sub>	251	0.67
N <sub>2</sub> O	418	0.5
O <sub>2</sub>	450	0.7
SO <sub>2</sub>	457	0.33
H <sub>2</sub> S	414	0.6

Paschen's curves for three gases, H<sub>2</sub>, Air and CO<sub>2</sub> are shown in Figure 2.3. These curves states that the relationship between breakdown voltages and product pd are not linear and all have a minimum value breakdown voltage corresponding to a  $(pd)_{min}$  value. The approximate pd value for air equals to 5 Torr-cm. If the  $pd < (pd)_{min}$ , electrons crossing the gap made only few collisions and higher voltage are needed to supply sufficient energy to the electrons to cause breakdown. When  $pd > (pd)_{min}$ , there are more frequent collisions between electrons and gas molecule than at  $(pd)_{min}$ , but electrons gain lower energy between collision, and the breakdown voltage for these conditions becomes higher than that of at  $(pd)_{min}$  values.

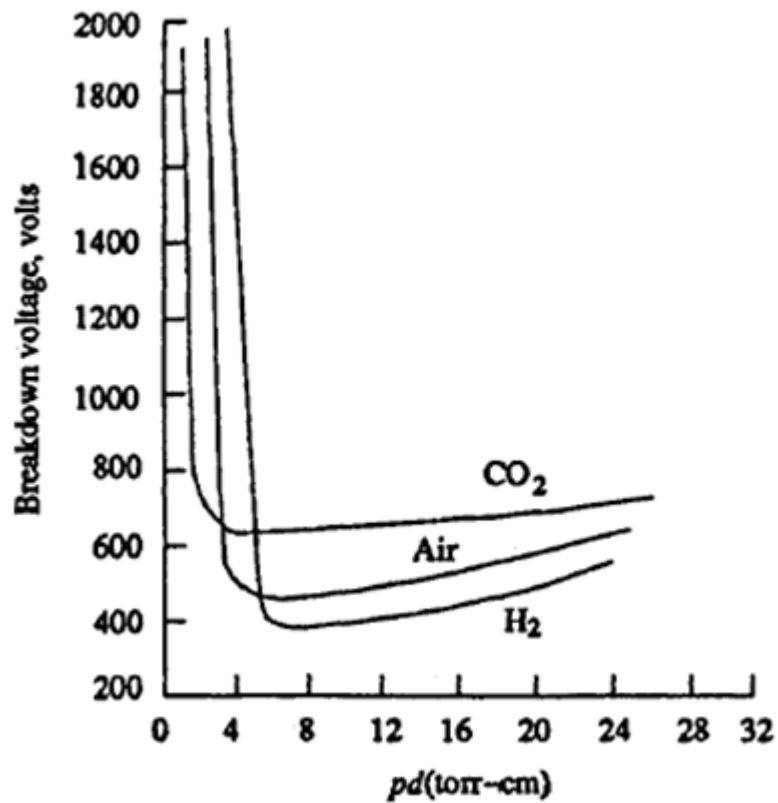


Figure 2.3 Paschen's law for breakdown voltages of H<sub>2</sub>, Air and CO<sub>2</sub>

Traditional aerospace system employ 400Hz frequency because the low frequency of switched frequency. Figure 2.4 shows the Paschen's curve at 400 Hz. Currently, the frequency in space systems is much higher than before, and Paschen's law still can be observed in kHz frequency system.

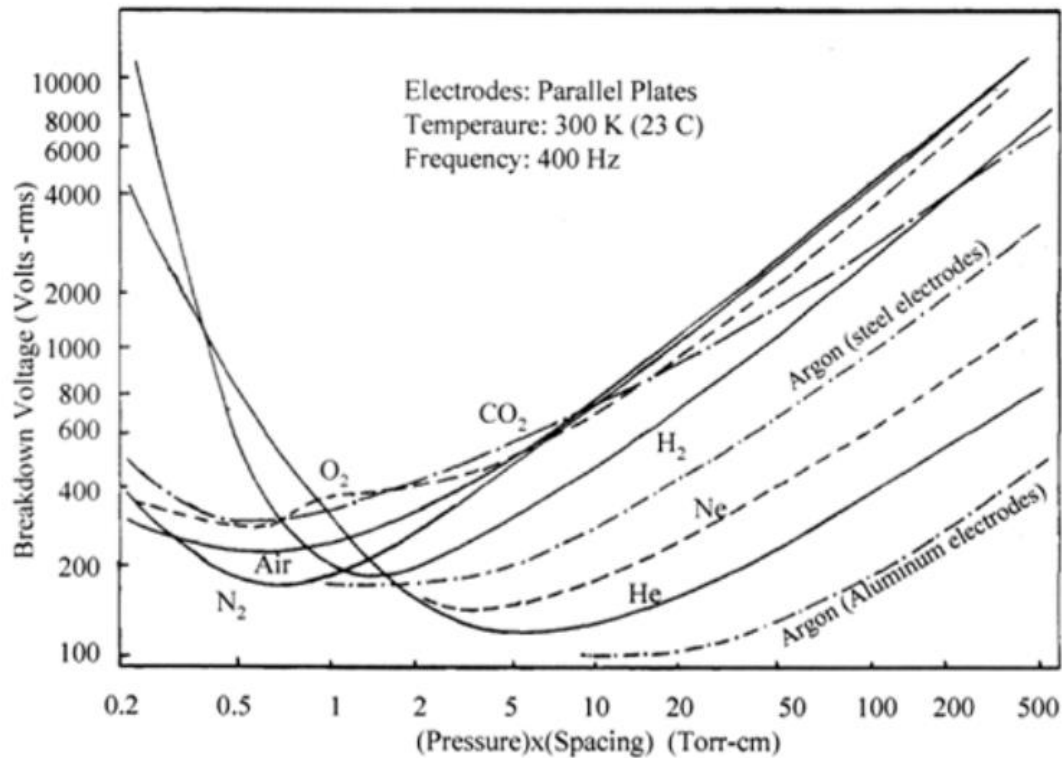


Figure 2.4 Paschen's curves of different gases under 400 Hz at room temperature [18]

### 2.2.3 Streamer Theory of Breakdown

Paschen's law has introduced the importance of  $pd$  in the breakdown process. The branched path and zigzag channel cannot be explained by Townsend theory under large  $pd$  values. In this case, streamer theory is presented to interpret these questions. The streamer process is shown in Figure 2.5.

Slow moving positive ions and fast moving electrons are generated when the electron avalanche happens. Positive ions are left behind; meanwhile electrons accumulate at the anode area. Atoms are excited by this primary avalanche and release photons in the gap. These photons are absorbed by the gas atoms at different places. This process produces ionization and photoelectrons (See Figure 2.5 a) and therefore generates the auxiliary avalanche.

The auxiliary avalanche, as the second avalanche, repeats above process and generates more photons and photoelectrons within the gap (See Figure 2.5 b). This stimulates more

auxiliary avalanches in coming period. But the space charge formed during this process distort the electrical field and simultaneous auxiliary avalanches form a zigzag patters from tip to tail (See Figure 2.5 c). With the developing of the avalanches, the spark channels are formed that connect the anode and cathode.

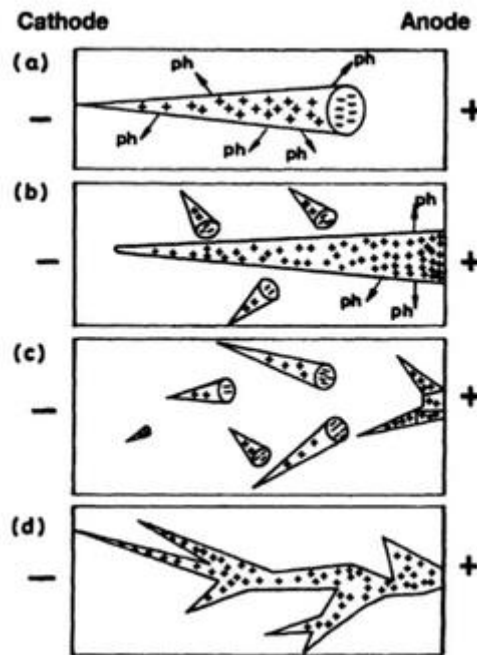


Figure 2.5 The development of avalanche to a streamer in a uniform field (+ = positive ions, - = electrons, ph = photons emitted from the avalanche [1])

### 2.3 High Frequency Breakdown

The discharge behavior becomes different as the frequency of the applied field reaches a relative high level. The maximum distance  $L_{max}$  lets all positive ions travel during a half-cycle of the applied is expressed as,

$$L_{max} = \int_0^{1/2f} k + \frac{V}{d} \sin 2\pi f t dt = \frac{k_+ V}{\pi f d} \quad (2.6)$$

Where  $V$  is the maximum amplitude of the applied voltage,  $d$  is the gap distance, and  $V/d \sin(2\pi ft)$  is the field strength. In this case, when  $d > L_{\max}$ , no positive ion cannot reach the opposite electrode during the half-cycle of the field. Then the Equation (2.6) can be revised to get a critical frequency  $f_c$ ,

$$f_c = \frac{k_+}{\pi d^2} V \quad (2.7)$$

When  $f < f_c$ , the breakdown characteristics is similar to statics field. When  $f > f_c$ , the positive ions will have no time to reach the cathode and oscillate in the gap. This accumulative charge will distort the field, increase the density of ions until avalanches happen. Due to the different mechanism, the breakdown under high frequency AC will occur at lower field strength than that under DC. This phenomenon are shown in Figure 2.6. Before positive ion oscillation, high frequency breakdown voltage is the same as under statics field. After that, the breakdown curve drops because of the field distortion until electron oscillation starts. Electrons will also not reach the anode during the half-cycle just like positive ions will not be able to get the cathode. Electrons oscillate between the electrodes to neutralize the positive ions and electrical field. This feature of breakdown forms the parabolic shape with increasing frequency [16].

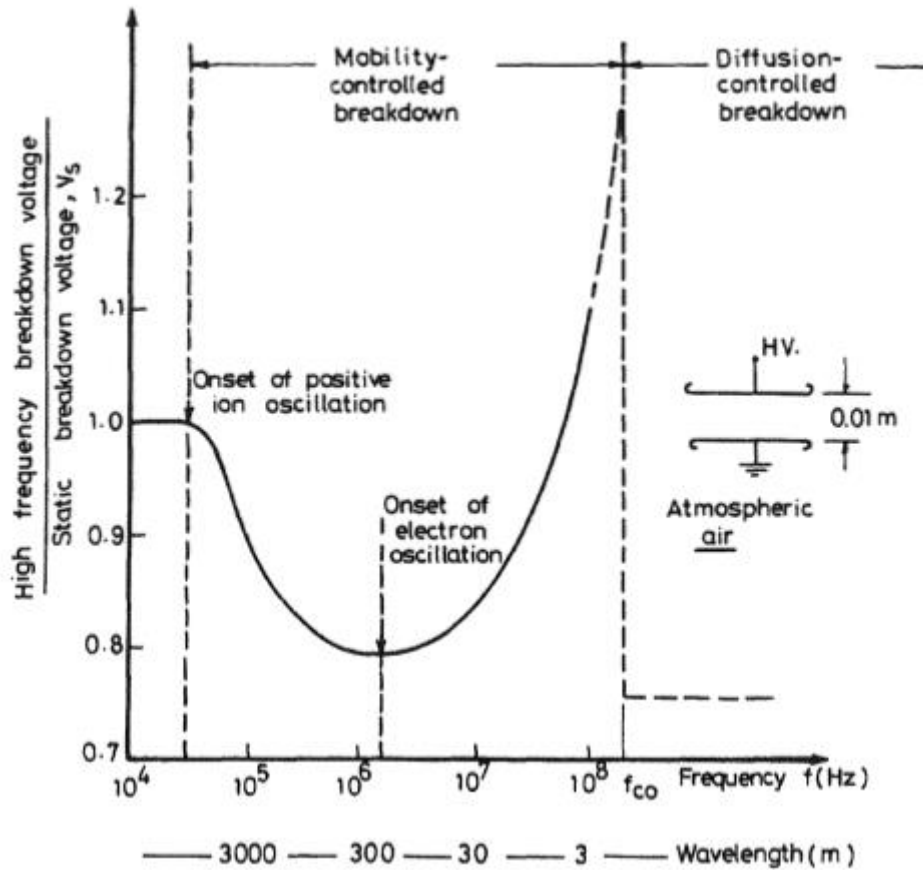


Figure 2.6 Ratio of high-frequency breakdown voltage to static breakdown voltage as a function of frequency for a uniform air gap [16]

## 2.4 Air and Gas dielectrics Insulation

### 2.4.1 Air Insulation Application

Due to the excellent insulating properties, air is mostly used as outdoor high voltage power system applications as well as insulation for indoor power systems. According to the practical applications in power system, air is often used to provide insulation protection for phase to phase as well as phase to ground. Therefore, different models are designed to simulate these different conditions. Table 2.2 summaries five kinds of commonly used models for power system insulation [1].

Table 2.2 Five kinds of models for investigation of different power networks [1]

Network section	Function	Model used for simulation
Phase to phase insulation	To provide insulation between two phases of an AC transmission line or between opposite poles of a bipolar DC line	Conductor- conductor, i.e., parallel cylinders or rod-plane electrodes to simulate the worst case of a sharp point on one conductor opposite to the other conductor
Phase to tower or phase to ground insulation	To provide insulation between the phase conductor and the grounded tower or the ground itself	Conductor- plane or rod-plane electrodes.
Small diameter conductor to grounded object insulation	To provide insulation between a sharp conductor and a flat grounded object in front of it. This type of geometry has the lowest air breakdown strength	Point- plane or rod- plane electrodes
Sphere-sphere gaps	High voltage measurements and high voltage switches in impulse generators	Sphere-sphere electrodes
High voltage protective or measuring gaps	To bypass high voltage surges to ground by a spark discharge. Also used for impulse chopping and for high direct voltage measurements	Rod-rod electrodes

#### 2.4.2 Gas Dielectrics

Due to the excellent properties of compactness, restorability and light weight, gases are widely utilized in space system and power system insulation. Each gas has a breakdown voltage at a specific pressure, temperature, and other parameters. Breakdown voltage is defined as the peak applied voltage across the electrodes when breakdown phenomenon occurs or spark channel forms. When DC voltage is applied across the electrodes, charged particles may be produced within the gap (see Figure 2.7). Such charged particles may include, electrons ( $e^-$ ), positive ions ( $A^+$ ) and negative ion ( $A^-$ ).

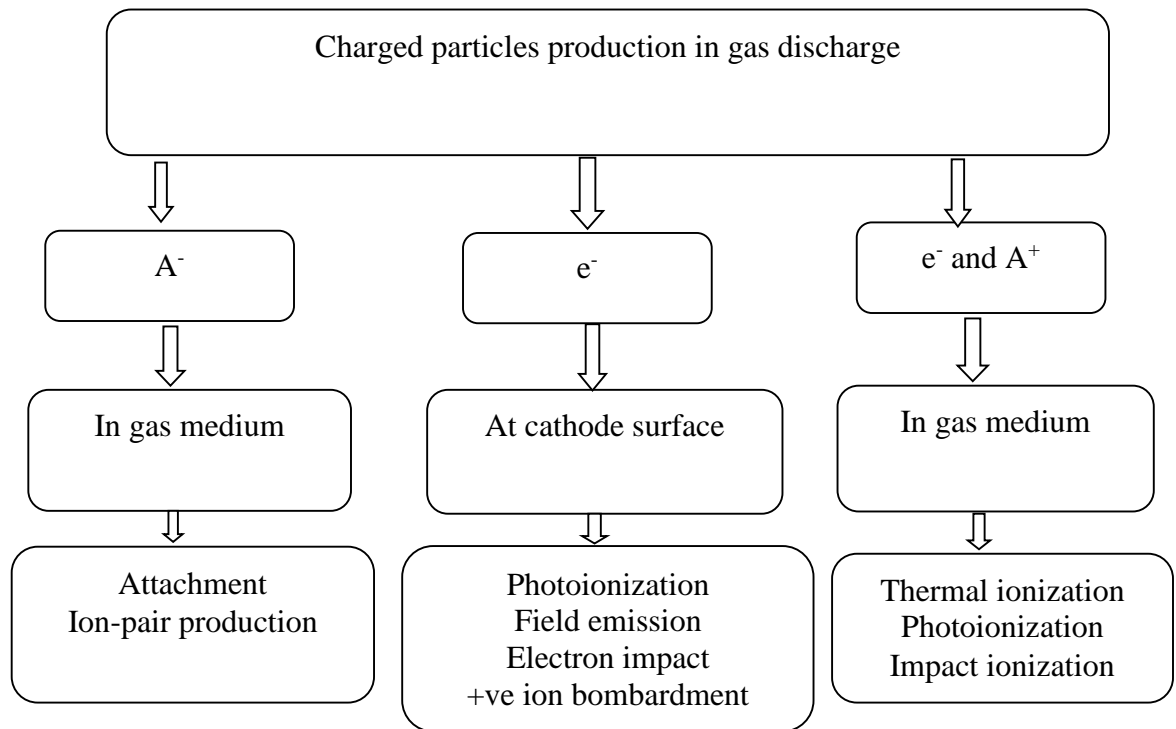


Figure 2.7 The main processes responsible for the production of the charged particles in a gas discharge

### 2.4.3 Vacuum Surface Flashover

Triple junction is an important mechanism for solid insulation surface flashover in vacuum. As shown in Figure 2.8, the junction part, the cathode metal, vacuum and solid insulator, is the most vulnerable part because of the different insulating properties of these materials, as well as the field enhancement at the junction. Emission of a single electron from the cathode tip as the initial electron, collides with the surface of the insulator to generate another electron. The initial and the secondary electrons continue to hit the dielectric surface, leading to an electron cascade and form an electron avalanche finally. This is the simple introduction to secondary electron emission avalanche (SEEA). When the electron flow reach the anode, the surface flashover will be completed.



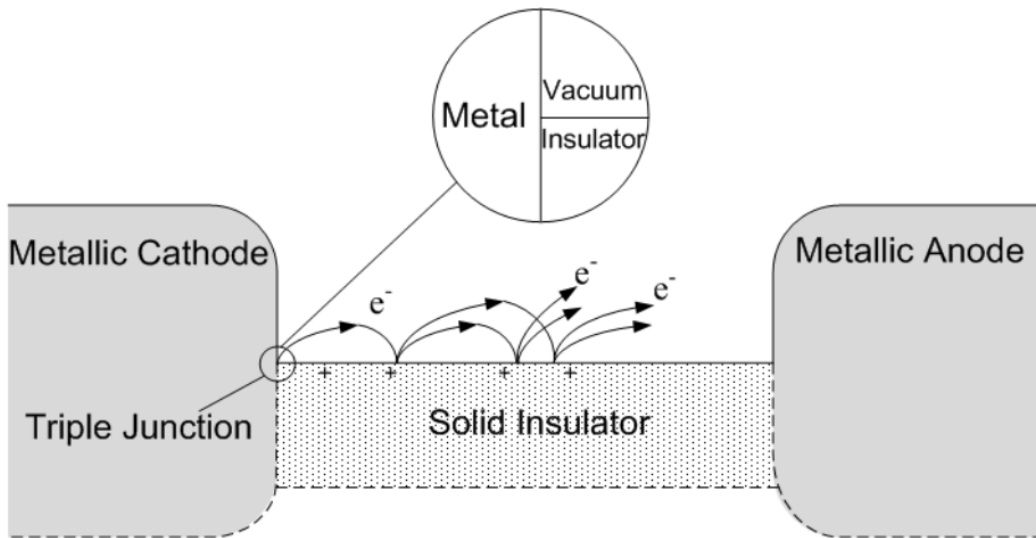


Figure 2.8 Schematic of triple junction in vacuum

The classical interpretation assumes that the intermediate stage of surface flashover is an electron cascade, and the final stage occurs in desorbed surface gas or in vaporized insulator material. The electron cascade can strongly affect the future development of SEEA.

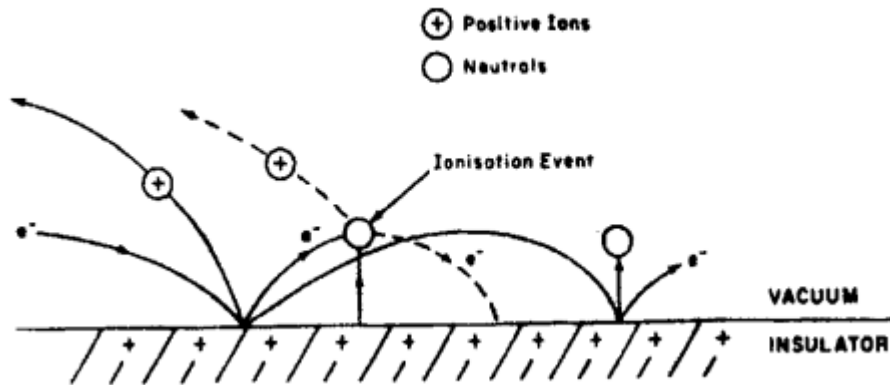


Figure 2.9 The mechanism of gas molecules are desorbed from the surface

Electron bombardment desorbs adsorbed gas which is ionized by the electrons (See Figure 2.9). Some positive ions drift toward the cathode. This process enhances the electrical field  $E$ . The enhanced electrical field will increase electron emissions from the triple junction further

and increase the current along the insulator surface. In this model, desorption of adsorbed gas is a key process leading to the surface flashover of an insulator.

## 2.5 Space System Insulation

Nowadays, space system needs high voltage and HV insulation (see Figure 2.10). In practice, the space environment is highly variable and anything but empty. Therefore, we need to consider many influences, such as residual gas, contamination, and etc. The most serious factors influencing electrical phenomena are the local radiation environment, thermal cycling, and local plasma density, neutral particle density, out gassing /effluents, and the meteoroid flux. In this thesis, only the breakdown of several gases at subatmospheric pressure, where most aerospace vehicles operate, is studied. Other space environmental effects are not studied.

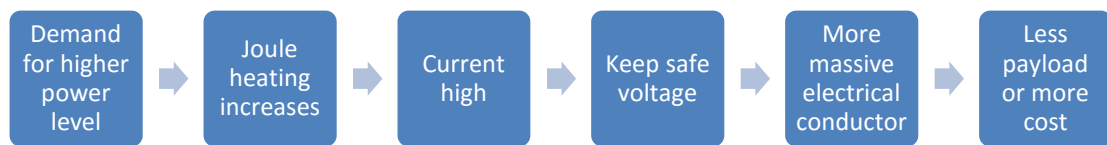


Figure 2.10 The needs for high power level space system

## **CHAPTER 3**

### **EXPERIMENTAL SETUP AND PROCEDURE**

#### **3.1 Experimental Setup**

The vacuum chamber is the main body of the experimental set-up (see Figure 3.1). The High Voltage (HV) probe, the current probe and the Photomultiplier (PMT) are connected to the experiment through different ports. HV probe is Tektronix p6015, to monitor the voltage inside the chamber. A Pearson Coil is used as the current probe, and encircle the wire that is connected to the anode in the chamber. The light emission from the plasma generated at breakdown is monitored by a Hamamatsu PMT. The current from the PMT is converted to voltage utilizing a Keithley 485 pico-ammeter. The light emission strength and voltage waveforms are display on the screen of an Agilent DSOX2012A digital oscilloscope (see Figure 3.2).

The light emission captured by PMT is used as the trigger signal to capture the breakdown voltage for the experiments. This is more reliable than the discharge current or negative slope of breakdown voltage. Therefore, shading the chamber form the outside light is necessary to avoid the influence of external light source on the PMT signal.

As we known, the breakdown phenomenon occurs instantaneously. Once the breakdown occurs, the oscilloscope will captured light emission strength and breakdown voltage data simultaneously.

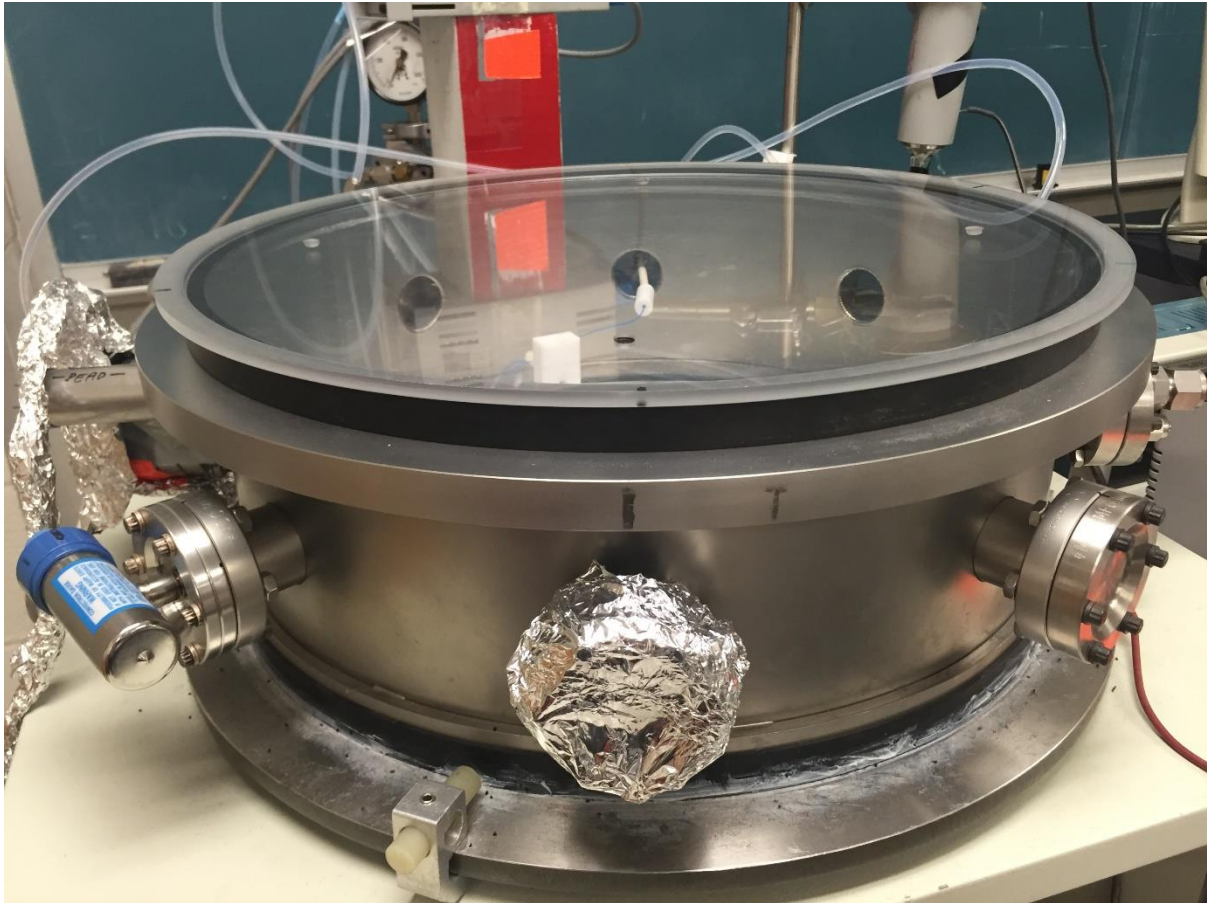


Figure 3.1 Vacuum Chamber

The point to point electrode geometry is one of the simplest configurations. As mentioned before, it is used to simulate phase-to-phase breakdown condition. The experimental set up consists of two needle-shape stainless steel electrodes that are placed 1 cm apart from each other as seen in Figure 3.3.

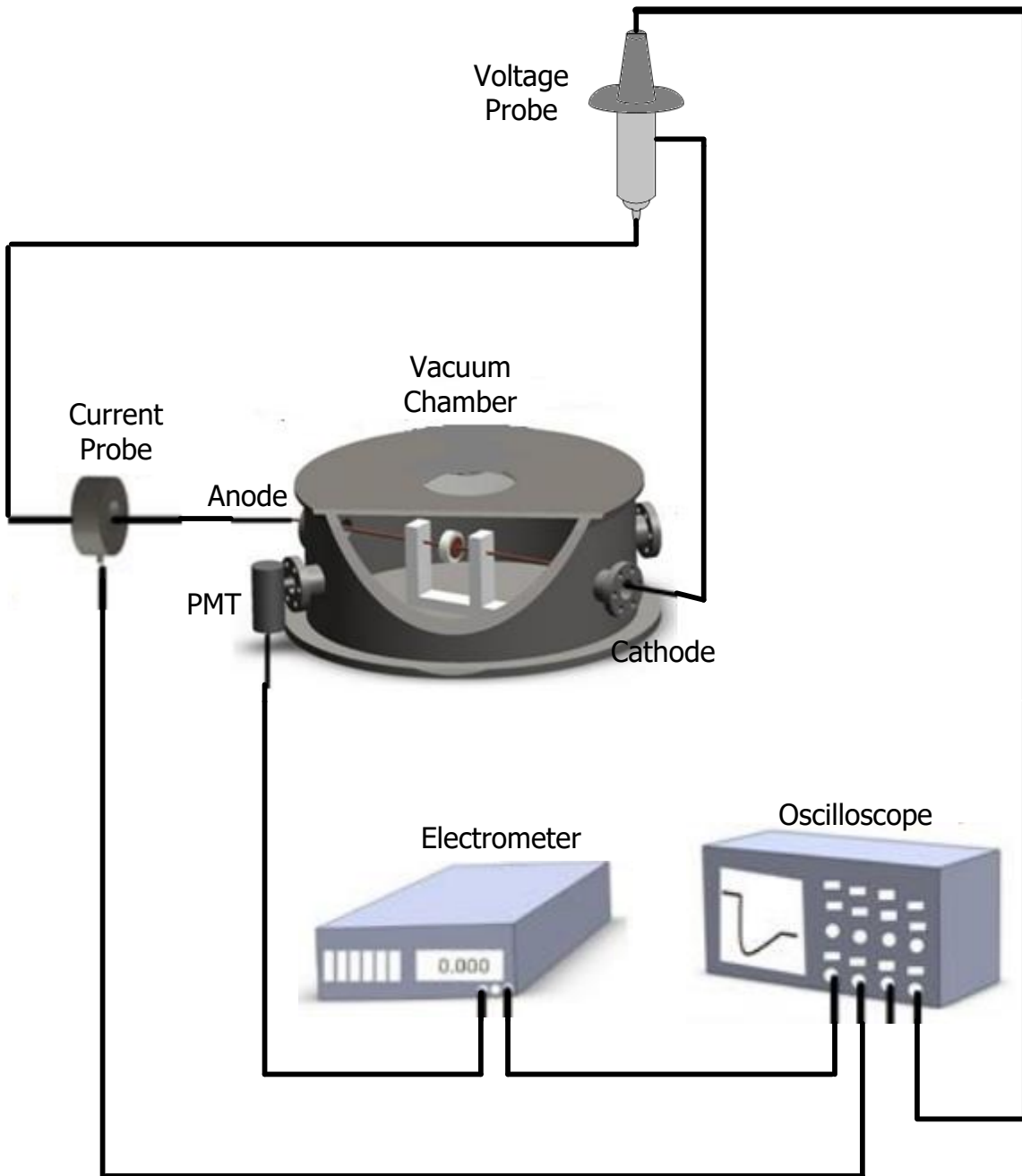


Figure 3.2 The schematic of the experiment setup

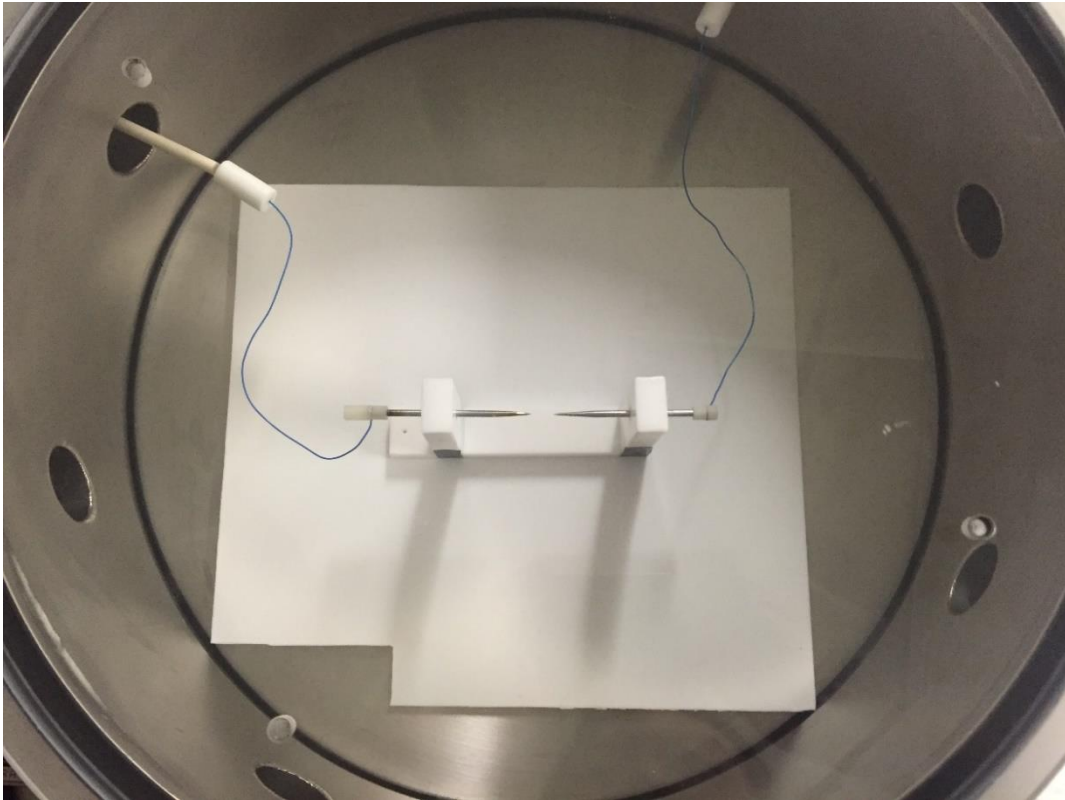


Figure 3.3 Point-to-point electrode configuration

### 3.2 Experimental Procedure

The experiments focus on the gas breakdown phenomenon. The breakdown voltage waveform data are recorded by the oscilloscope for each pressure then a set of data is generated as the breakdown voltage versus pressure. The experiments are conducted under partial vacuum environment, mainly at the range of 100 milliTorr to 10 Torr. Before every set of experiments, it is necessary to bump the chamber until the chamber pressure is below 100 milliTorr, then fill in the corresponding gas to satisfy the pressure requirement. In the pressure sweep experiments, at a constant pressure, the DC voltage is applied between the electrodes and increased at a constant rate (about 100V/s) from 0 volts to until the breakdown occurs. The pressure ranges are from minimum level of 100 milliTorr to different upper pressure level. Air and Nitrogen are common gases, therefore their experimental pressure range will be 100 milliTorr to 2 Torr. The experiments with argon gas is under 100 milliTorr to 5 Torr. But Helium being the second lightest element in nature, therefore, pumping the chamber down to vacuum level and refilling at each fixed pressure value is necessary to record correct breakdown data. Also, it is know that the Paschean minimum occurs at about 5 too-cm, the upper pressure for helium breakdown experiments reaches 10 Torr. For every fixed pressure value of each gas, four breakdown data points are acquired. The average value of these repeated data reduces the error effectively.

## CHAPTER 4

### RESULTS AND DISCUSSION

#### 4.1 Theoretical Calculation

The experiments are the primary stage of understanding the high-voltage insulation. It is important to understand the meaning of Townsend theory and Paschen's law. According to these two significant theories, we can get the theoretical calculation results to plot the breakdown voltage curve versus pressure of gases. Every curve should have its own Paschen curve and  $(pd)_{\min}$  point. This theoretical curve will be the reference for the real experimental result.

Reviewing the content mentioned in Chapter 2, the equations can be rewrite as:

$$\frac{\alpha}{p} = A \exp\left(-\frac{B}{E/p}\right) \quad (4.1)$$

Where  $\alpha$  is the Townsend coefficient,  $p$  is the pressure and  $E$  is the electrical field.  $A$  and  $B$  are specific constants and given in Table 3.1 for each gas studied.

Table 4.1 Numerical Parameters  $A$  and  $B$  of Townsend Coefficient  $\alpha$

Gas	$A$ , 1/cm Torr	$B$ , V/cm Torr
Air	15	365
N <sub>2</sub>	10	310
He	3	34
Ar	12	180

The breakdown voltage as a function of the important parameter  $pd$ :

$$V = \frac{B(pd)}{C + \ln(pd)} \quad (4.2)$$



B is provided by Table 31, and is given by  $C = \ln A - \ln \ln (1 + 1/\gamma)$ .

It is convenient to calculate the breakdown voltage if the Townsend secondary ionization coefficient  $\gamma$  is known. Townsend secondary ionization coefficient  $\gamma$  depend on type of gas, cathode material, and reduced electrical field  $E/p$ . This value of  $\gamma$  is measurable, but varies for different materials and gases. Typical range of  $\gamma$  is 0.01~0.1 [19]. We select  $\gamma=0.1$  for this calculation. Thus, it is enough to calculate all the breakdown voltages as follows below and shown in Figure 4.1. With the data of Figure 4.1, a Paschen curve can be plotted.

One important point needed to notice is that the values of A and B are empirical, based on many stable previous studies. But they are valid only between 1-10 Torr approximately. Because the Townsend breakdown theory is mainly focus on glow charge and is valid in this pressure range. The theory breakdowns at pressure below 100 milliTorr. That is exactly the reason for negative values in the charts (figure 4.1). These negative values will be neglected during plotting the Paschen curves.

Figure 4.1, 4.2, 4.3, and 4.4 show the calculations of breakdown voltages of air, nitrogen, helium, and argon respectively. In the valid pressure range, all figures show a good match with well-known Paschen curve.

Table 4.2 Calculation Process of Air Breakdown Voltage (A=15 1/cm Torr, B=365 V/cm Torr)

pd(Torr cm)	d(cm)	$\gamma$	C	Air Breakdown Voltage (V)
0.13	1	0.1	1.833459	-229.491
0.15	1	0.1	1.833459	-860.022
0.2	1	0.1	1.833459	325.8624
0.3	1	0.1	1.833459	173.9514
0.4	1	0.1	1.833459	159.1857
0.5	1	0.1	1.833459	160.044
0.6	1	0.1	1.833459	165.5788
0.8	1	0.1	1.833459	181.331
1	1	0.1	1.833459	199.0773
2	1	0.1	1.833459	288.9251
3	1	0.1	1.833459	373.4562
4	1	0.1	1.833459	453.4509
6	1	0.1	1.833459	604.1016
8	1	0.1	1.833459	746.2495
10	1	0.1	1.833459	882.4858
15	1	0.1	1.833459	1205.546
20	1	0.1	1.833459	1511.64

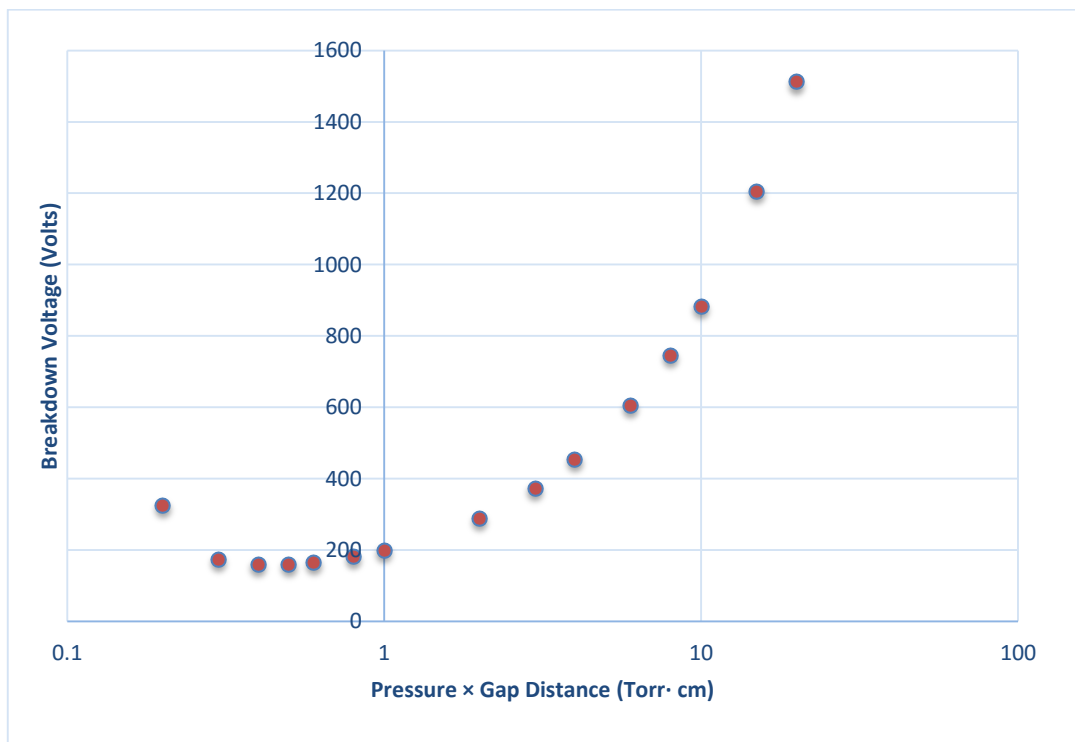


Figure 4.1 Air Breakdown Voltage as a Function of Pressure with Theoretical Data

Table 4.3 Calculation Process of Nitrogen Breakdown Voltage (A=10 1/cm Torr, B=310 V/cm

Torr)

pd(Torr cm)	d(cm)	$\gamma$	C	Nitrogen Breakdown Voltage (V)
0.01	1	0.1	1.427994	-0.97571
0.26	1	0.1	1.427994	996.0447
0.27	1	0.1	1.427994	705.3744
0.3	1	0.1	1.427994	415.1398
0.4	1	0.1	1.427994	242.3281
0.5	1	0.1	1.427994	210.9284
0.6	1	0.1	1.427994	202.7982
0.8	1	0.1	1.427994	205.8347
1	1	0.1	1.427994	217.0878
2	1	0.1	1.427994	292.2955
3	1	0.1	1.427994	368.0827
4	1	0.1	1.427994	440.6088
6	1	0.1	1.427994	577.684
8	1	0.1	1.427994	707.0694
10	1	0.1	1.427994	830.9702
15	1	0.1	1.427994	1124.263
20	1	0.1	1.427994	1401.533

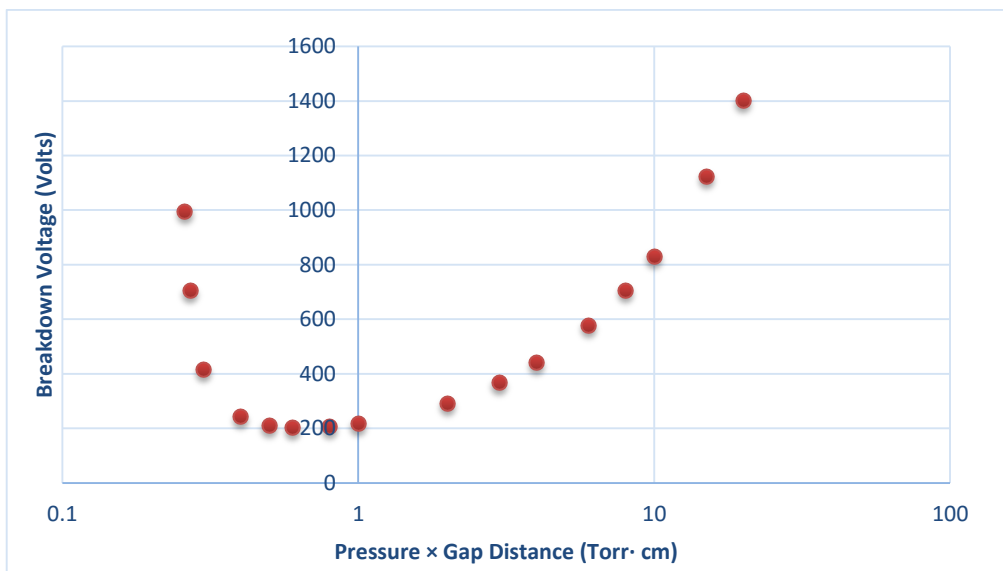


Figure 4.2 Nitrogen Breakdown Voltage as a Function of Pressure with Theoretical Data

Table 4.4 Calculation Process of Helium Breakdown Voltage (A=3 1/cm Torr, B=34 V/cm

Torr)

pd(Torr cm)	d(cm)	$\gamma$	C	Helium Breakdown Voltage (V)
0.01	1	0.1	0.224021	-0.06752
0.1	1	0.1	0.224021	-1.24391
0.2	1	0.1	0.224021	-3.33307
0.3	1	0.1	0.224021	-6.23968
0.4	1	0.1	0.224021	-10.0964
0.65	1	0.1	0.224021	-25.6527
0.7	1	0.1	0.224021	-30.226
0.8	1	0.1	0.224021	-41.5985
1	1	0.1	0.224021	-78.9365
2	1	0.1	0.224021	259.1251
3	1	0.1	0.224021	152.7205
4	1	0.1	0.224021	142.3236
6	1	0.1	0.224021	149.8861
8	1	0.1	0.224021	164.9769
10	1	0.1	0.224021	181.6376
15	1	0.1	0.224021	223.947
20	1	0.1	0.224021	265.1065

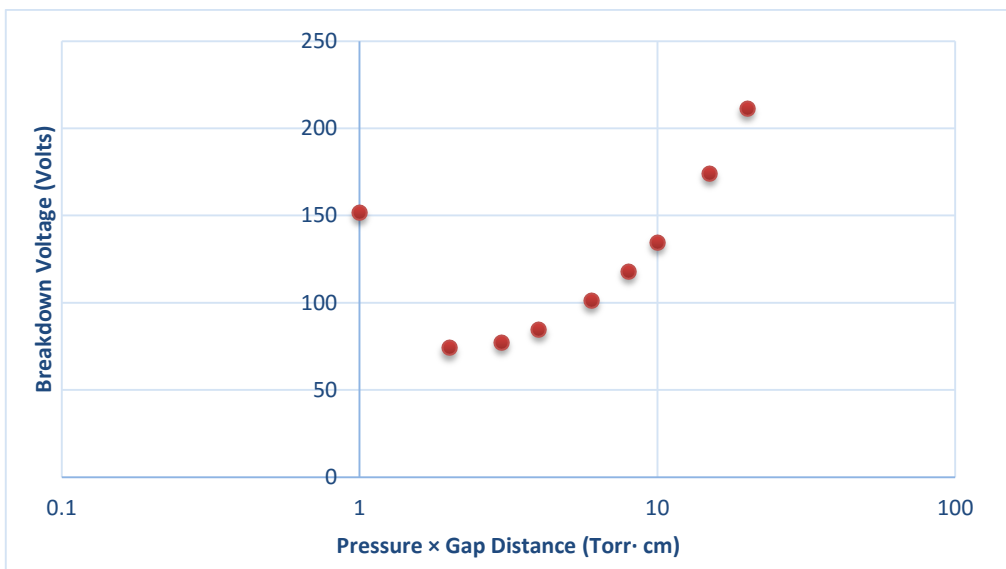


Figure 4.3 Helium Breakdown Voltage as a Function of Pressure with Theoretical Data

Table 4.5 Calculation Process of Argon Breakdown Voltage (A=12 1/cm Torr, B=180 V/cm

Torr)

pd(Torr cm)	d(cm)	$\gamma$	C	Argon Breakdown Voltage (V)
0.16	1	0.1	0.955569	-129.574
0.17	1	0.1	0.955569	-189.308
0.2	1	0.1	0.955569	41032.45
0.3	1	0.1	0.955569	132.8928
0.4	1	0.1	0.955569	103.7427
0.5	1	0.1	0.955569	98.12814
0.6	1	0.1	0.955569	98.22739
0.8	1	0.1	0.955569	103.8083
1	1	0.1	0.955569	111.7794
2	1	0.1	0.955569	156.2865
3	1	0.1	0.955569	199.3409
4	1	0.1	0.955569	240.2715
6	1	0.1	0.955569	317.4533
8	1	0.1	0.955569	390.2696
10	1	0.1	0.955569	460.0168
15	1	0.1	0.955569	625.2366
20	1	0.1	0.955569	781.5812

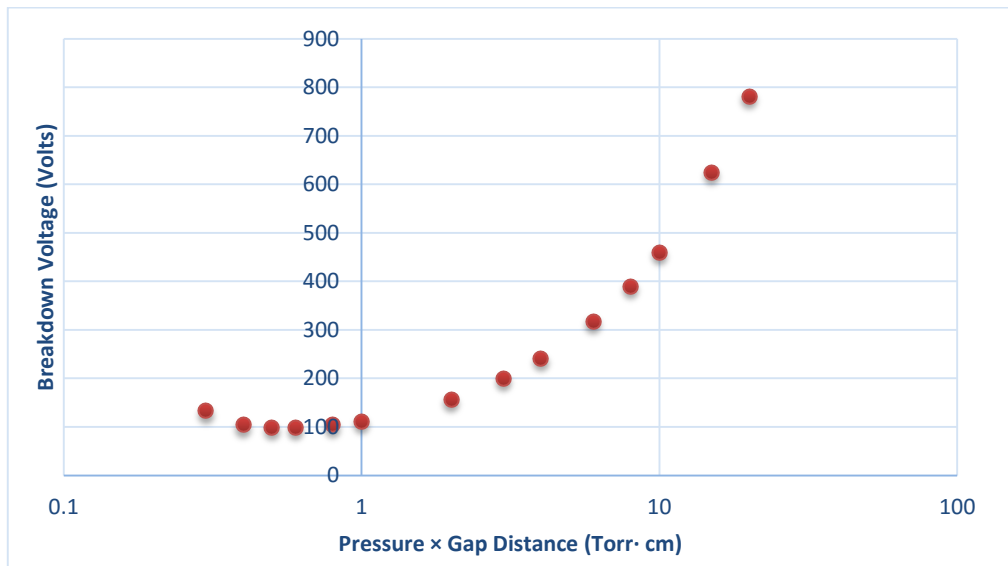


Figure 4.4 Argon Breakdown Voltage as a Function of Pressure with Theoretical Data

## 4.2 DC Breakdown Experiments

As described in Chapter 3, DC voltage is applied across the electrodes, increased gradually with a rate of 100 V/s, until the breakdown phenomenon occurred. The plasma initiation light emission is recorded by the PMT (shown in Figure 4.5 yellow bottom line). The acquisition system triggered by positive slope edge of light signal and used to capture the breakdown voltage signal. Therefore, these two signals displayed on the screen. In order to decrease the errors, the experiments under same pressure was repeated four times. The average value of these four data is the breakdown voltage for its corresponding pressure. Similar experiments were conducted in air, nitrogen, helium, and argon. Specially, in the experiments of helium, because its property of light mass, it is necessary to pump the chamber down at the beginning of every pressure. Even though, satisfactory data cannot be obtained easily. Therefore, a second set of helium breakdown voltage experiments was conducted to ensure the accuracy of first set of data.

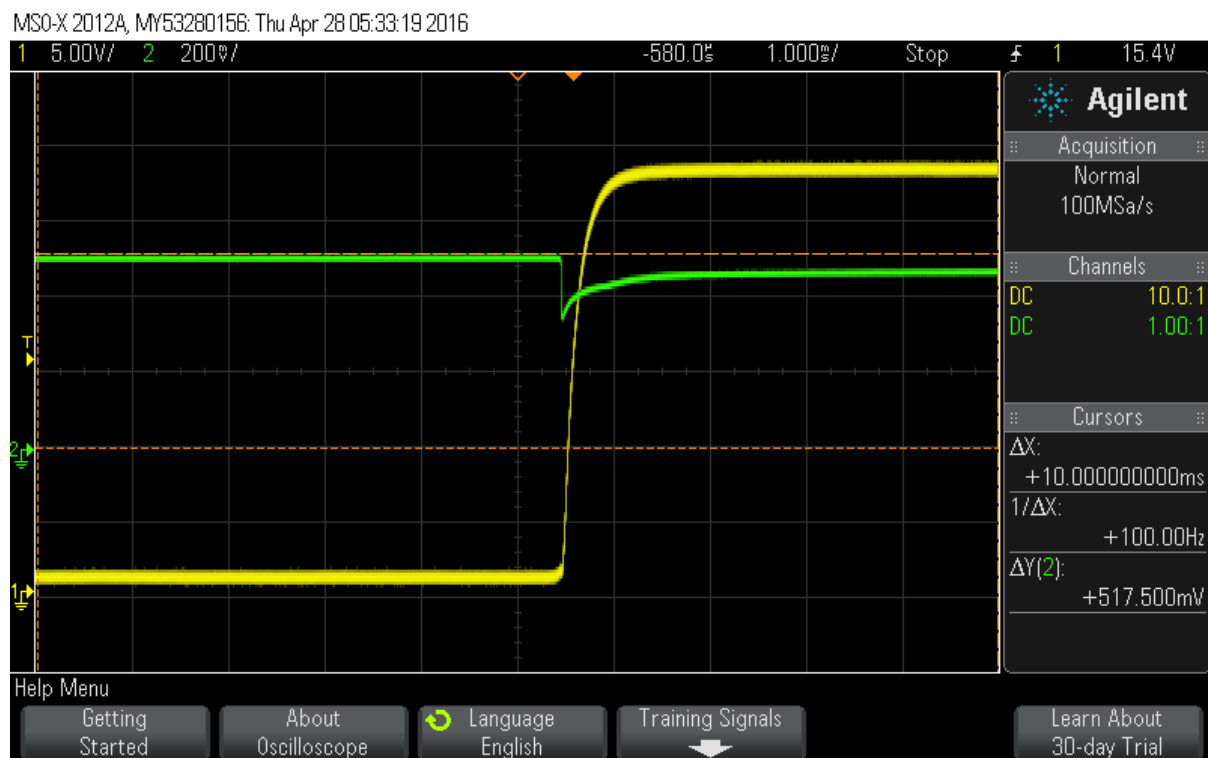


Figure 4.5 Voltage (top), light emission (bottom) waveforms of a breakdown event point-to-point electrode geometry for DC voltage at 100 milliTorr

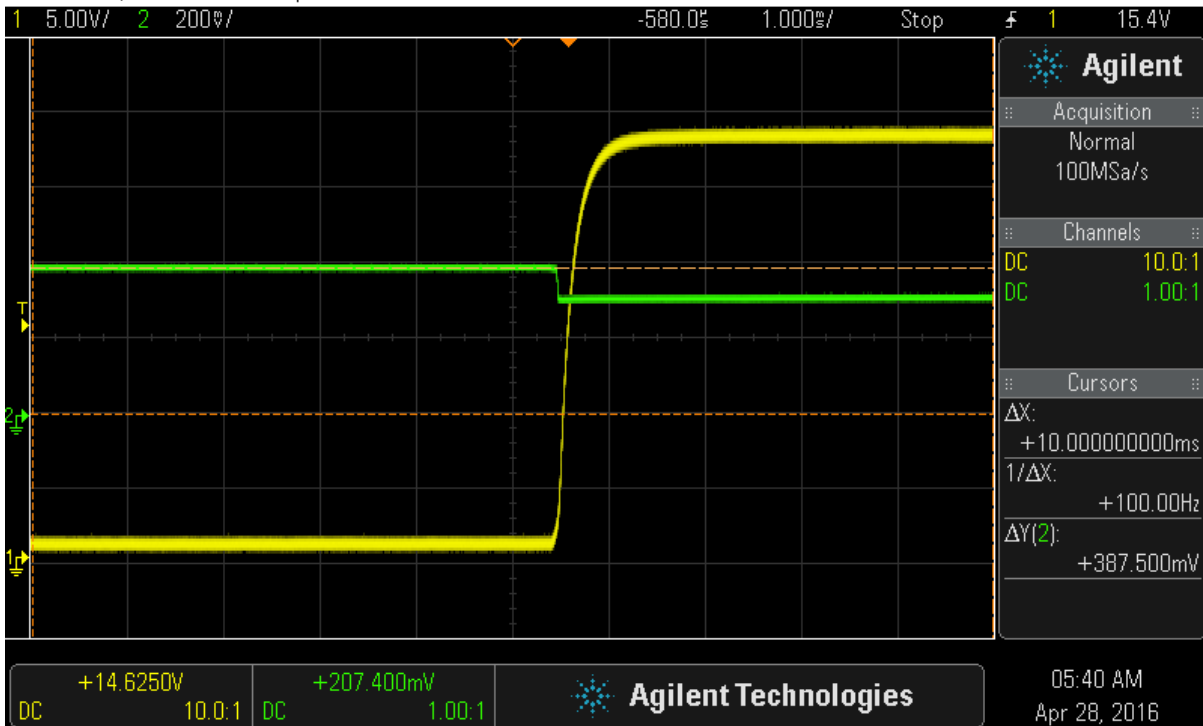


Figure 4.6 Voltage (top), light emission (bottom) waveforms of a breakdown event point-to-point electrode geometry for DC voltage at 6 Torr

Figure 4.7 shows the air breakdown voltage curve. This is a right hand side of the Paschen curve with obvious rising up tendency. Its  $p d_{\min}$  appears at 100~200 milliTorr. If extend the left part of this curve to far less than 100 milliTorr, it should have a significant high breakdown voltage value. Between the range of 100 milliTorr to several Torr, air has an excellent insulating property, its lowest breakdown voltage is still more than 640 V.

Figure 4.8 shows the nitrogen breakdown voltage curve. Its breakdown curve resembles the Paschen curve with both positive and negative slope. Although the values at 400 and 600 Torr·cm distort the bottom part of this curve, it is still complete and a good curve to show the insulating properties in this range.

Figure 4.9 (a) has two seems to be in error at 2.4 Torr and 3 Torr. Because of the special properties of helium, the breakdown voltage values from 1 Torr to 8 Torr fluctuate at a stable

region. Only if the pd reach to more than 10 Torr, the breakdown voltage could have a rising up tendency. Because of the limitation of pressure gauge, the voltage at more than 10 Torr was not measured in this experiment. The curve of Figure 4.9 (b) is similar to Figure 4.9 (a). That means no severe error occur in our experiments and the overall shape of curve is correct.

Figure 4.10 shows the argon breakdown voltage curve. It has a good configuration of curve. Its  $pd_{min}$  is about 800 ~1000 miliiTorr, which is match the  $pd_{min}$  provided by Table 2.1.

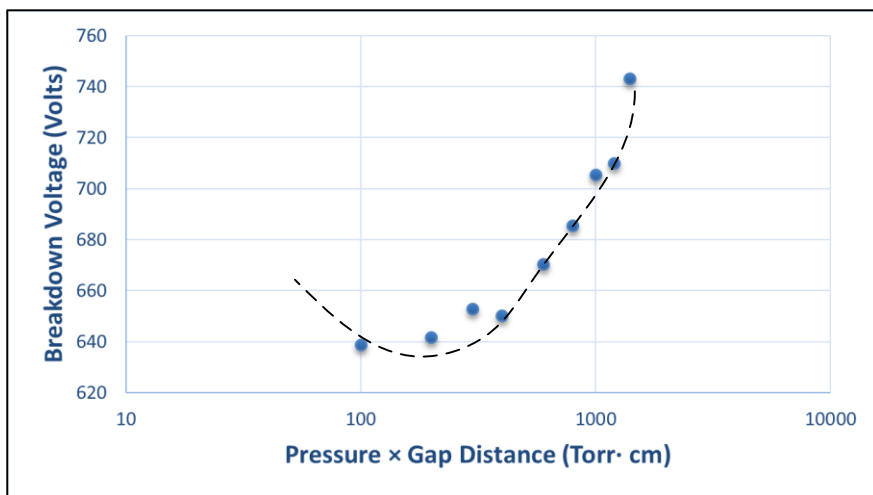


Figure 4.7 Air Breakdown Voltage as a Function of Pressure with Experimental Data

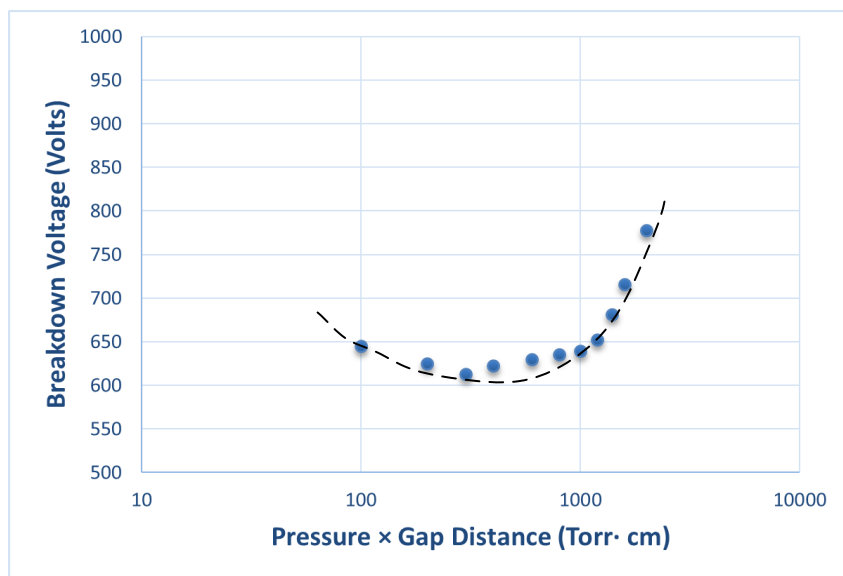


Figure 4.8 Nitrogen Breakdown Voltage as a Function of Pressure with Experimental Data



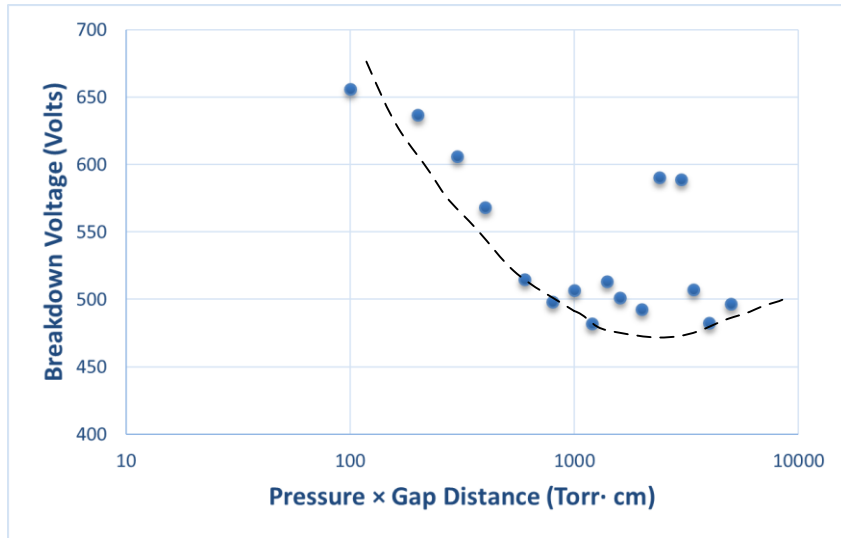


Figure 4.9 Helium Breakdown Voltage as a Function of Pressure with Experimental Data (a)

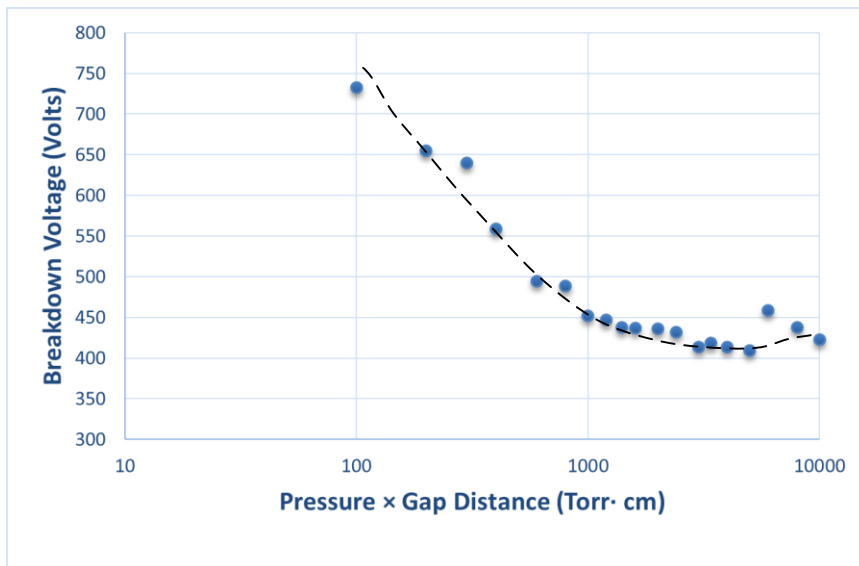


Figure 4.10 Helium Breakdown Voltage as a Function of Pressure with Experimental Data (b)

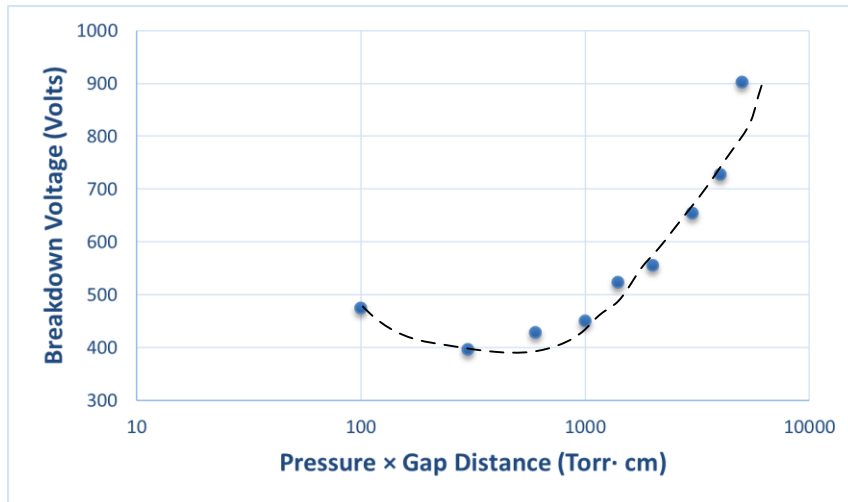


Figure 4.11 Argon Breakdown Voltage as a Function of Pressure with Experimental Data

### 4.3 Comparison between Theoretical and Experimental Curves

Figures 4.12, 4.13, 4.14, and 4.15 show the comparison of theoretical and experimental breakdown voltages of air, nitrogen, argon, and helium respectively. Compared to the experimental curve with theoretical curve in the same coordinate system, these two curves have same tendency at most pd point, but with a constant shift in voltage values. That is because the theoretical curve are based on the uniform electrical field, the  $\gamma$  and value of A and B are constant under the prediction of uniform electrical field. But the point-to-point electrodes have only nonuniform electrical field. It seems like reasonable to have a constant difference value. The detail reason for this phenomenon need future research in the future.

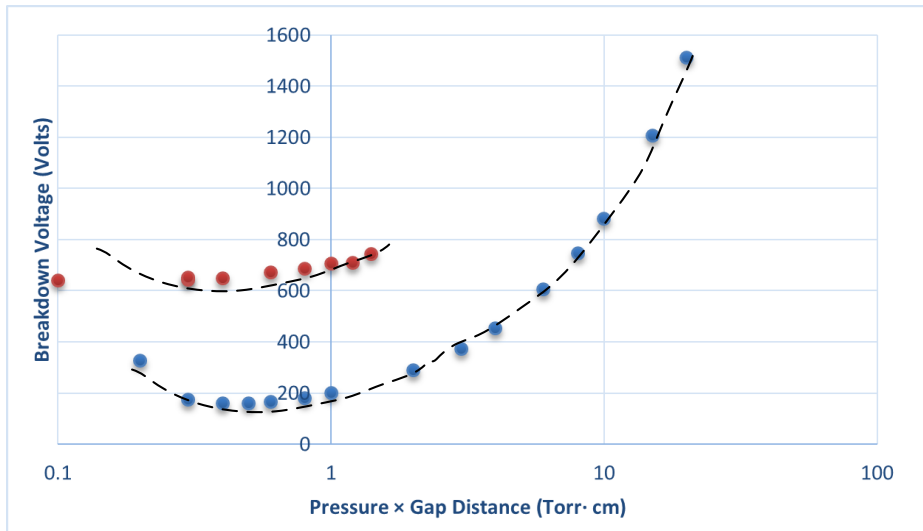


Figure 4.12 Comparison between Theoretical and Experimental Air Breakdown Voltage Curve (Experimental top, Theoretical bottom)

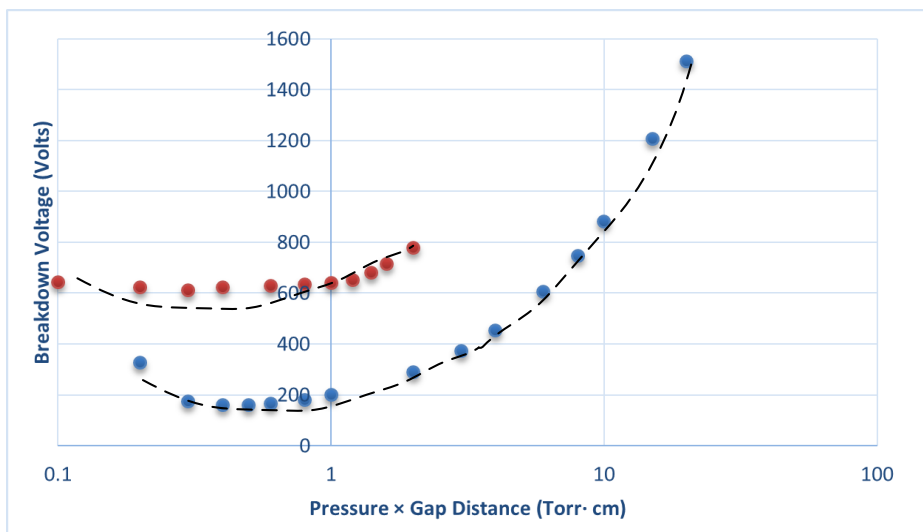


Figure 4.13 Comparison between Theoretical and Experimental Nitrogen Breakdown Voltage Curve (Experimental top, Theoretical bottom)

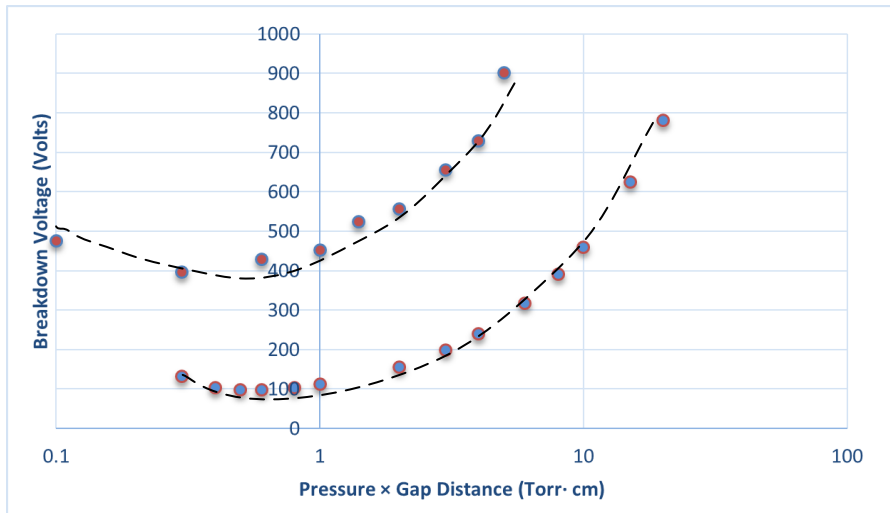
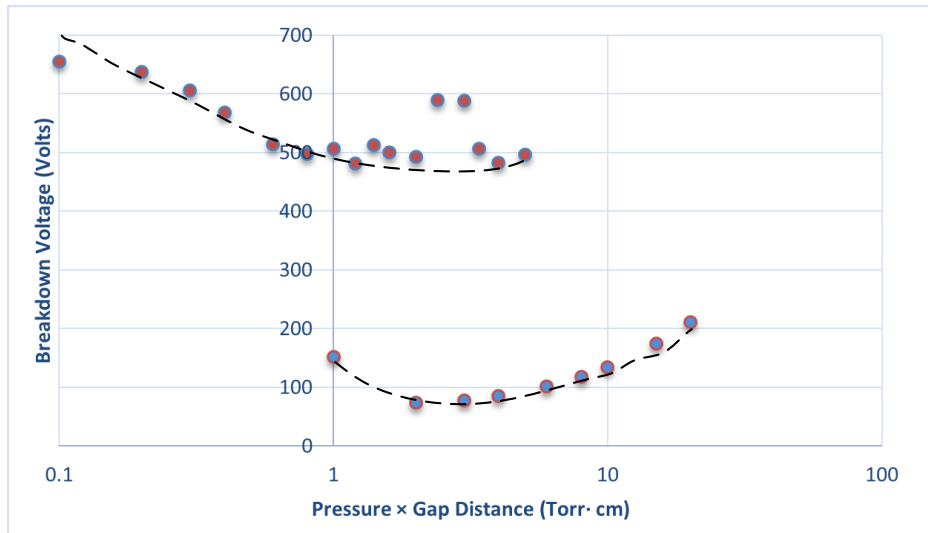
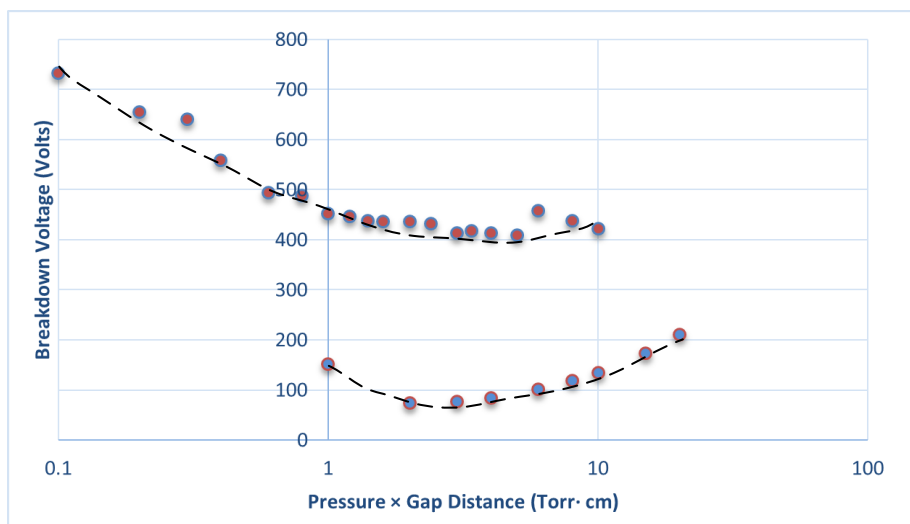


Figure 4.14 Comparison between Theoretical and Experimental Argon Breakdown Voltage Curve (Experimental top, Theoretical bottom)



(a)



(b)

Figure 4.15 Comparison between Theoretical and Experimental Helium Breakdown Voltage  
Curve (a) first time (b) second time

#### 4.4 Summary

This study I introduced the method to calculate the breakdown voltages for four gases with Paschen's law and Townsend theory. Then the experimental study is conducted confirming the correctness of our calculation under DC applied voltage.

Theoretical calculation is based on Townsend secondary ionization coefficient  $\gamma$ , which depends on the type of gas, cathode material, and reduced electrical field  $E/p$ . This value of  $\gamma$  is set at 0.1 in this calculations for all four different gases. The breakdown voltage is a function of pressure under DC voltage. They also have a parabolic curve like Paschen curve without the influence of error data.

Experiments confirms the existence Paschen curve between 100 milliTorr and several Torr. It also shows the breakdown voltage is a function of pressure. Because the difference of applied electrical field, uniform electrical field for theoretical and nonuniform one for experimental, theoretical and experimental breakdown voltage curves have same tendency at most pd point, but with a constant shifted voltage value. The experiments are successful to confirm the consistency between theoretical and experimental breakdown voltage curves.

## CHAPTER 5

### CONCLUSIONS

This thesis is mainly consist of two parts, one is theoretical calculation, and the other one is experimental confirmation. It clarifies the correlation between two different research methods for gas breakdown phenomenon study. Gaseous dielectrics is the simplest insulation material for power system. Study with gas dielectrics is also the initial stage and necessary way to research on solid dielectrics. Familiar with the basic breakdown mechanism is benefit for learning with plasma and micro- or nano- dielectrics. This experiment utilized point-to-point electrode, to simulate conditions of high voltage protective or measuring gaps.

In the first part, this theoretical calculation is based on Townsend breakdown theory and utilized the secondary ionization coefficient  $\gamma$ , which depends on type of gas, cathode material, and reduced electrical field  $E/p$ . It is convenient to calculate the breakdown voltage if we know the Townsend secondary ionization coefficient  $\gamma$  for the gases in our experiments. But for the sake of calculating an acceptable set of data, we set  $\gamma$  equal to 0.1 for all four gases in this experiment. With the data of calculation, a Paschen curve can be drawn out easily. The values of A and B used for calculation are empirical, based on many stable previous studies and are valid only between 1-10 Torr approximately (glow discharge region). Before plotting the breakdown voltages versus pressure curve, negative voltage values were deleted and removed from the calculations. Finally, from the figures of theoretical calculation, it can be realized that the breakdown voltage is a function of pressure under DC voltage. These figures own a parabolic curve like Paschen curve when neglect the influence of error data.

As the second part of this thesis is the experimental study of breakdown of gases to confirm the existence Paschen curve between 100 milliTorr and several Torr. It also shows the breakdown voltage is a function of pressure. Because the difference of applied electrical field, uniform electrical field for theoretical and nonuniform one for experimental, theoretical and experimental breakdown voltage curves have same tendency at most  $pd$  point, but with a constant difference value. The experiments successfully confirm the consistency between theoretical and experimental breakdown voltage curves. Besides, the nitrogen and argon have perfect Paschen curve in this pressure range under DC applied voltage. Nitrogen and air have the largest breakdown voltage value at their  $pd_{min}$ . It is worth mentioning that their  $pd_{min}$  appear at what the supposed to be. Conduction and ground are important prospects for this experiment. Without stable wire conduction, flashover phenomenon occurred between two wires rather than at the gap of two electrodes. We have tried copper wire, stainless steel wire until Teflon wire is utilized in this experiment. Also, bad connection to absolute ground will lead to the reference potential inaccuracy.



## REFERENCES

- [1] Malik, N., Al-Arainy, A. and Qureshi, M. (1998). *Electrical insulation in power systems*. New York: Marcel Dekker.
- [2] F. Hegeler, H. Krompholz, L. Hatfield and M. Kristiansen, "Dielectric surface flashover in a simulated low Earth orbit environment", *IEEE Trans. Plasma Sci.*, vol. 25, no. 2, pp. 300-305, 1997.
- [3] Meng Wang, "Investigations of surface flashover of insulators in vacuum and applications of vacuum insulators in pulsed power system", *XXIst International Symposium on Discharges and Electrical Insulation in Vacuum, 2004. Proceedings. ISDEIV*.
- [4] M. Serkan, H. Kirkici and K. Koppisetty, "Surface Flashover Characteristics of Nano Particle Cast EPOXY Resin", *2005 IEEE Pulsed Power Conference*, 2005.
- [5] W. Zhao, G. Zhang, Y. Yang and Z. Yan, "Correlation between trapping parameters and surface insulation strength of solid dielectric under pulse voltage in vacuum", *IEEE Transactions on Dielectrics and Electrical Insulation*, vol. 14, no. 1, pp. 170-178, 2007.
- [6] P. Yan, T. Shao, J. Wang, W. Gao, W. Yuan, R. Pan, S. Zhang and G. Sun, "Experimental investigation of surface flashover in vacuum using nanosecond pulses", *IEEE Transactions on Dielectrics and Electrical Insulation*, vol. 14, no. 3, pp. 634-642, 2007.
- [7] Y. Chen, Y. Cheng, J. Tang, K. Wu, Y. Sun, L. Shao, Q. Chen, W. Yin, Z. Wang and J. Zhou, "Experiments and Simulations on Influencing Factors of Pulsed Surface Flashover in Vacuum", *2007 IEEE International Conference on Solid Dielectrics*, 2007.
- [8] Y. Cheng, Y. Chen, P. Tang, K. Wu, L. Shao, Q. Chen, Y. Sun, W. Yin, Z. Wang and J. Zhou, "Study on the Vacuum Surface Flashover Characteristics of Epoxy Composites with Different Fillers under Steep High-Voltage Impulse", *2007 IEEE International Conference on Solid Dielectrics*, 2007.
- [9] Z.B. Wang, Y.H. Cheng, Y. Chen, M. Ding, J.B. Zhou, G.D. Meng and K. Wu, "Study on the Vacuum Surface Flashover Characteristics of Epoxy Composites with MicroTiO<sub>2</sub> Fillers under Steep High-Voltage Impulse", *2007 IEEE International Conference on Solid Dielectrics*, 2007.
- [10] Yong-Hong. Cheng, Zeng-Bin. Wang and Kai. Wu, "Pulsed Vacuum Surface Flashover Characteristics of TiO<sub>2</sub>/Epoxy Nano-Micro Composites", *IEEE Transactions on Plasma Science*, vol. 40, no. 1, pp. 68-77, 2012.
- [11] Zhenhong. Li and Hulya. Kirkici, "Surface flashover of nanodielectrics with varying electrode architectures in partial vacuum under DC and kHz pulsed fields", *2012 IEEE International Power Modulator and High Voltage Conference (IPMHVC)*, 2012.

- [12] Mark. Lipham, Haitao. Zhao and Hulya. Kirkici, "Breakdown characteristics of Argon in partial vacuum under high frequency pulsed voltage with varying duty cycle", *2009 IEEE Pulsed Power Conference*, 2009.
- [13] A. Boudjella, H. Hadi, M. Yumoto, T. Sakai and T. Hosokawa, "Investigation on discharge development phenomena on D.C. high voltage insulator of two grooves", *2000 Annual Report Conference on Electrical Insulation and Dielectric Phenomena*, 2000.
- [14] K. Koppisetty, H. Kirkici and D. Schweickart, "Partial vacuum breakdown characteristics of helium at 20 kHz for inhomogeneous field gap", *IEEE Transactions on Dielectrics and Electrical Insulation*, vol. 14, no. 3, pp. 553-559, 2007.
- [15] Le. Xu, Meng. Wang, Feng. Li, Zun. Yang and Jianjun. Deng, "Spectroscopic Study of Surface Flashover Under Pulsed Voltage in Vacuum", *IEEE Trans. Plasma Sci.*, vol. 43, no. 10, pp. 3546-3549, 2015.
- [16] Abdel-Salam, M., Anis, H., El-Morshedy, A. and Radwan, R. (2000). *High-voltage engineering*. New York, N.Y.: Marcel Dekker.
- [17] Haddad, A. and Warne, D. (2004). *Advances in high voltage engineering*. London: Institution of Electrical Engineers.
- [18] E. Hastings, G. weyl, Guy and D. Kaufman, "Threshold voltage for arcing on negatively biased solar arrays", *Journal of Spacecraft and Rockets*, vol. 27, pp. 539-544, 1990.
- [19] Fridman, A. and Kennedy, L. (2004). *Plasma physics and engineering*. New York: Taylor & Francis.